SPE-200329-MS

Crude Oil/Brine/Rock Interactions during SmartWater Flooding in Carbonates: Novel Surface Forces Apparatus Measurements at Reservoir Conditions

Kai Kristiansen, University of California Santa Barbara; Roberto C Andresen Eguiluz, Unveristiy of California Merced; Szu-Ying Chen, University of California Santa Barbara; Subhash C Ayirala, Mohammed B Alotaibi, and Ali A Yousef, Saudi Aramco; Martin Moskovits, James R Boles, and Jacob N Israelachvili, University of California Santa Barbara

This paper was prepared for presentation at the SPE Improved Oil Recovery Conference originally scheduled to be held in Tulsa, OK, USA, 18 – 22 April 2020. Due to COVID-19 the physical event was postponed until 31 August – 4 September 2020 and was changed to a virtual event. The official proceedings were published online on 30 August 2020.

Abstract

In our previous paper (SPE-190281-MS), we presented results from a suite of multiscale experiments to understand interactions occurring across crude oil/brine/carbonate rock interfaces with different brine compositions. A new atomic to molecular scale mechanism was proposed based on changes in adhesion energies at different length- and time-scales to explain SmartWater effects for improved oil recovery (IOR) in carbonates. It was also understood that SmartWater effect is due to three distinct but interrelated physico-chemical mechanisms, involving changes to the colloidal interaction forces, surface roughening due to dissolution and re-precipitation, and removal of pre-adsorbed organic-ionic ad-layers (termed 'flakes') from the rock surface.

In the present study, we carried out surface forces apparatus (SFA) experiments to understand SmartWater IOR mechanisms at elevated temperatures and pressures (up to 150°C and 2,200 psi) representative of realistic reservoir conditions. The results of earlier SFA measurements at elevated temperature showed a significant dependence of SmartWater effect on temperature, while the dependence of pressure still remained unexplored. To overcome this major shortcoming and fill the missing gap in existing knowledge, a unique High Pressure-High Temperature Surface Forces Apparatus (HPHT-SFA) has been designed with the same surface visualization capabilities as regular SFA (nm normally and μm laterally).

The calcite thickness and roughness changes measured using the HPHT-SFA at elevated pressures showed a significant difference between SmartWater flooding versus high salinity water (HSW) flooding. During SmartWater flooding, a high rate of removal of organic-ad layer from the aged calcite surface (manifested by a substantial decrease in the layer thickness) and an unexpected degree of smoothening of calcite (i.e., decrease in the difference between the maximum and minimum thicknesses of calcite) were observed. The change in maximum thickness (i.e., thickness of flakes removed) was found to be around 100 nm, consistent with measurements at atmospheric pressure. The rate of flake removal from carbonate surface

with SmartWater, however, was aggravated at high pressures when compared to that observed at atmospheric conditions. Another set of experiments revealed that under high pressures HSW flooding was not able to remove organic flakes from aged calcite surface, in contrast to analogous results obtained at ambient pressure. These findings suggest that not only temperature has strong effect governing the restructuring of the calcite surface, but also the pressure plays an important role affecting the kinetics of organic layer detachment from the calcite surface.

This study presents first ever results obtained from the newly designed HPHT Surface Forces Apparatus to demonstrate the importance of elevated pressures on crude oil/brine/rock interactions in SmartWater flooding. The novel findings obtained at reservoir temperature and pressure conditions are of practical significance to provide a better understanding of SmartWater flooding IOR mechanisms and subsequently guide the optimization of SmartWater flooding processes in carbonate reservoirs.

Introduction

The SmartWater effect is a promising route to increase oil recovery in both sandstone[1-4] and carbonate reservoirs[5-11] and it looks much attractive over other IOR/enhanced oil recovery (EOR) techniques especially involving surfactant chemicals[12-17] due to its simplicity and cost-effectiveness. The SmartWater composes of low-salinity brine water with tailored ionic compositions that upon flooding in reservoirs causes the migration of fines (or flakes of organic-ionic adlayers), changes on pH, and wettability[18-21], resulting in detachment and retrieval of crude oil[22]. Figure 1 shows the proposed mechanism of the SmartWater effect[23], where upon injection of low salinity brine water with sufficient amounts of three key ions (sulfate, calcium, and magnesium), the crude oil-rock adhesion is weakened by removal of interstitial flakes and roughening of the carbonate rock surface[24]. Moreover, the SmartWater increases the van der Waals repulsion between the crude oil and rock surface. Most of the experimental laboratory studies reported so far have focused on the effect of salinity and ionic compositions, and less on the effect of temperature and even less on the effect of hydrostatic pressure. However, the two latter contributions to IOR are of crucial importance to better understand and distinguish the key phenomena occurring at realistic reservoir conditions.

In this work, we present a new design of a Surface Forces Apparatus that works under high temperature and high-pressure conditions. In addition, a Contact Angle measurement mechanism is included in the design. We find that the unexplored territory of laboratory experiments under high pressure provides new and unexpected results, which has significant impact on the molecular understanding of increased oil recovery using SmartWater flooding.

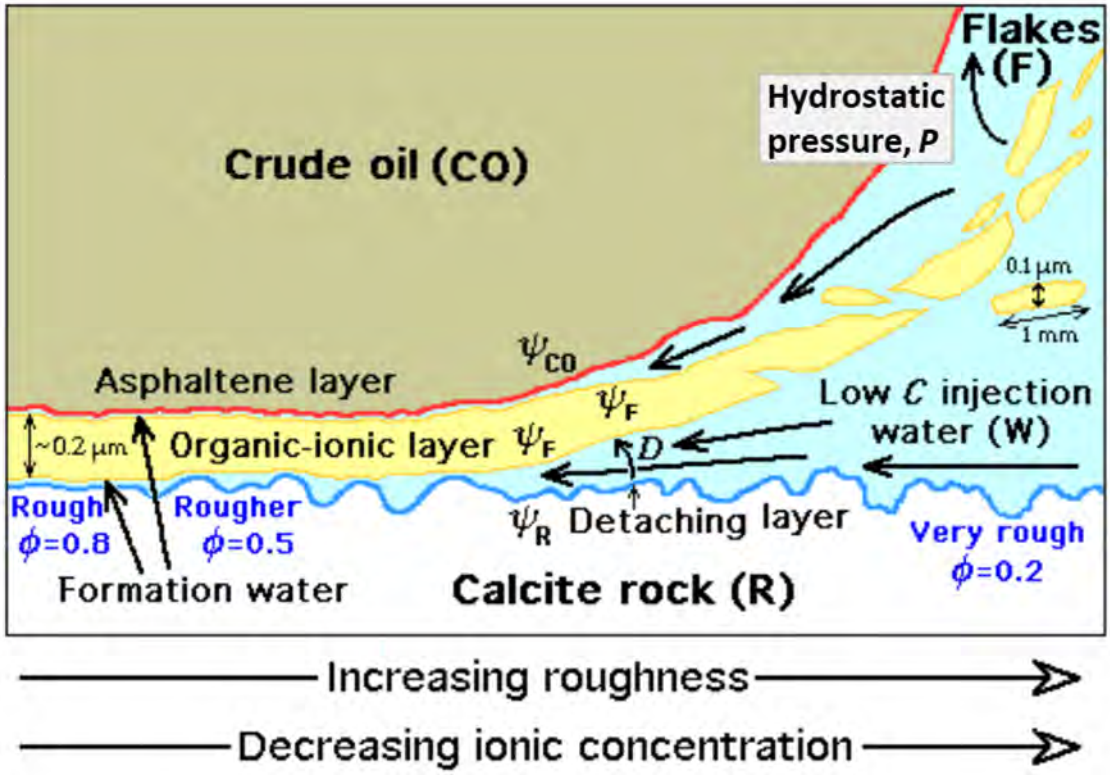

Figure 1—Mechanisms of the SmartWater Effect. The ψ values refer to the surface potentials, which determine the colloidal interaction forces; the symbol of C denotes the concentration of the brine solution; P is the hydrostatic pressure in the solution; the φ values are the surface roughness parameters for the effective surface area of the calcite exposed to the brine solution. Our main question is, what is the effect of hydrostatic pressure on the SmartWater effect? (Adapted from SPE-190281-MS[24]).

Materials and Methods

Sample and solution preparation

Materials. The calcite rock samples were synthesized in-house from solution using previously published protocols[23]. The stocktank degassed crude oil (CO) sample was obtained from a carbonate reservoir with its SARA composition, total acid number, and other properties presented in Table 1. The field brine solutions were re-constructed in laboratory using deionized (DI) water (18.2 MΩ·cm; Millipore Milli-Q) and reagent grade salt chemicals (sodium chloride, calcium chloride, magnesium chloride, sodium sulfate, and sodium bicarbonate; Sigma-Aldrich). Table 2 gives the composition of the synthesized formation water (FW) and high salinity water (HSW). Compositions were based on geochemical analyses of field water samples obtained from the same carbonate reservoir. The SmartWater solution has a concentration 1/10th of the concentration of HSW to retain sufficient amounts of three key ions (sulfates, calcium, and magnesium), and was prepared by mixing HSW with the appropriate amount of DI water. Table 3 shows the saturation indices for the different calcium-containing minerals in the different brine solutions were calculated using the PHREEQC aqueous modeling software with a pH 6 solution at 100 °C referenced against the oxygen redox standard. All brine solutions were filtered using 0.2 μm polypropylene-based syringe filters (Anotop 10 IC) prior to use in experiments.

Table 1—Properties of the crude oil[23].

Components (%)	**Saturates**	39.2
	Aromatics	48.3
	Resins	7.0
	Asphaltenes	5.5
Total Acid Number (mg KOH/g oil)		0.25
Stock tank oil gravity at 60°F (°API)		34.1
Dead oil density at STP (lb/ft^3)		54.5
Dead oil viscosity at STP (cP)		14.6

Table 2—Geochemical analyses of reservoir formation water (FW) and injected high salinity water (HSW), and composition of SmartWater ([HSW]/10 solution)[23].

Ions	Formation Water (FW) [ppm]	High Salinity Water (HSW) [ppm]	SmartWater [ppm]
Sodium	59,500	18,300	1830
Calcium	19,000	650	65
Magnesium	2,400	2,100	210
Sulfate	350	4,300	430
Chloride	132,000	32,200	3,220
Bicarbonate	350	120	12
Total Dissolved Solids (TDS)	**214,000**	**58,000**	**5,800**

Table 3—Saturation indices for the different calcium-containing minerals in the different brine solutions[24].*

Solution**	Calcite	Aragonite	Dolomite	Anhydrite	Gypsum
Formation water	1.1	1.0	1.8	0.3	-0.3
High salinity water (HSW)	-0.5	-0.6	-0.4	-0.1	-0.5
SmartWater ([HSW]/10 solution)	-2.1	-2.2	-3.5	-1.2	-1.6

*Calculated using the PHREEQC aqueous modeling software with a pH 6 solution at 100°C referenced against the oxygen redox standard.

**Mineral species that are undersaturated have negative saturation indices and are highlighted in dark grey. Mineral species that are oversaturated have positive saturation indices and are highlighted in light grey.

Calcite Surface Conditioning Procedure[23]. The experiments followed a two-step calcite surface conditioning procedure (see Figure 2). In Step 1, referred to as the aging step, a clean calcite sample was equilibrated with FW that had been pre-saturated with CO surfactants (FW-CO) in a sealed container at 100°C for 24 h to restore the original reservoir wettability of the calcite surface. FW-CO was prepared by equilibrating FW with CO (1 FW:1 CO by volume) in a sealed glass vial at 100°C for 24 h and then extracting the FW from the two-liquid solution. After undergoing the aging step, the resultant sample was thereafter referred to as being 'fully-aged'. In Step 2, referred to as the 'SmartWater Effect' step, fully-aged calcite was equilibrated with the different experimental reservoir brine solutions (*e.g.*, HSW and SmartWater solutions) in the sealed HPHT-SFA container to study the effects of reducing the ionic strength of the injection SmartWater on the CO/W/R system. Depending on the experiment, different components of the samples were subsequently extracted for experiments and analyses.

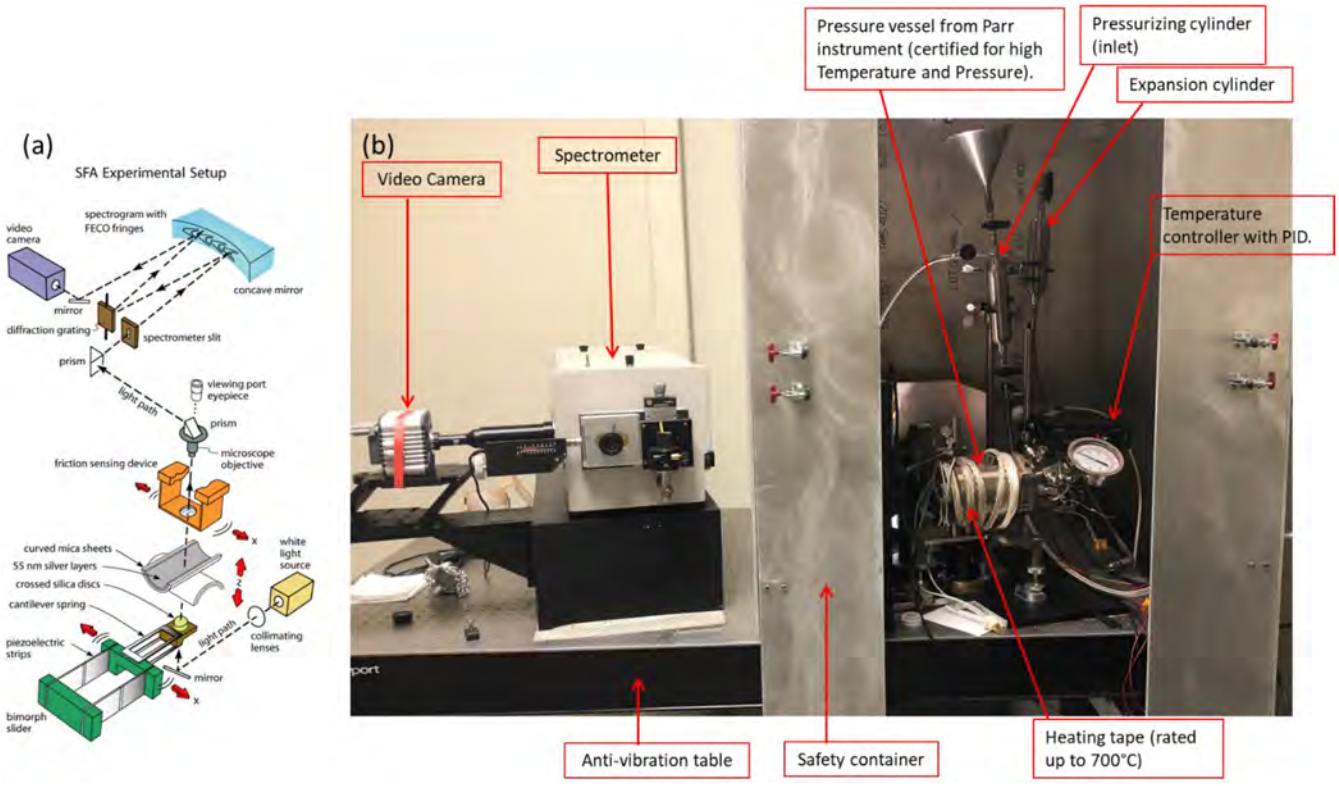

Figure 2—The high temperature-pressure contact angle and surface forces apparatus (HTHP-SFA) experimental setup. (a) Schematic of the standard SFA experimental setup showing the light interferometric technique and how the mica surfaces are moved using piezoelectric (bimorph) strips. (b) Photo of the HTHP-SFA setup where the pressure vessel is heated using a heating tape controlled with a PID controller, and the pressure tubes pressurize the pressure vessel using a high-pressure nitrogen gas cylinder (not shown) and safety shield for protection. Complete and tested for pressures up to 150 atm. and high temperatures of 150°C. (The transparent shield in front provides a complete safety container, but is not present).

The High Temperature-High Pressure Surface Forces Apparatus (HTHP-SFA)

Surface Forces Apparatus (SFA). The SFA technique uses white light interferrometry to monitor in real time the calcite thickness and morphology[25]. A measure of the calcite evolution during waterflooding is the maximum and minimum thickness of the combined two apposing calcite surfaces in the contact region (for schematic, see inset in Figure 7).

The design of the HTHP-SFA. Figure 2 shows the experimental setup of the HTHP-SFA, in which several modifications were carried out as compared to the standard SFA (e.g., SFA 2000)[26]. These include: (1) a newly designed chamber that allows measurements at high temperature and pressure to be carried out, see Figure 3, (2) develop a new method for moving the sample surfaces laterally and normally, see Figures 4 and 5, (3) that is intended to allow for an *in-situ* Contact Angle setup, see Figure 5, and (4) to develop a pressurizing system and safety shield, see Figure 2, respectively. The custom-designed pressure vessel was purchased from and certified by Parr Instruments, while the rest of the HTHP-SFA is built in our laboratory. The heating of the HTHP-SFA is done using heating tape (heavy duty rated up to 700 °C) with a precision to within 2 °C. Heating and pressurization were successfully implemented.

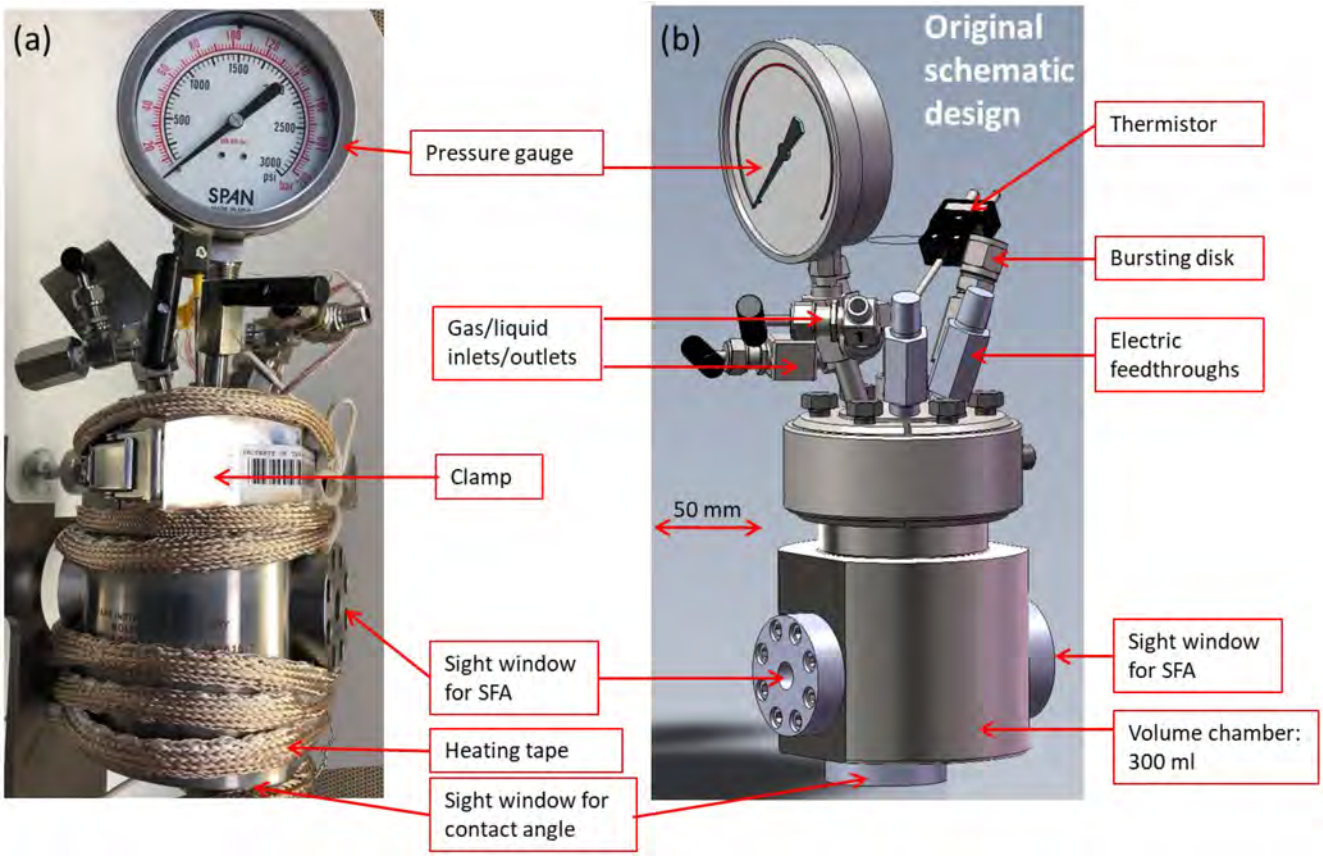

Figure 3—The pressure vessel for the HTHP-SFA. (a) A photo and (b) the schematic of the pressure vessel purchased from Parr Instrument Co. This is certified to withstand 3000 PSI (204 atm) and 225°C. Our new design of the Surface Forces Apparatus and Contact Angle device fits inside this pressure vessel.

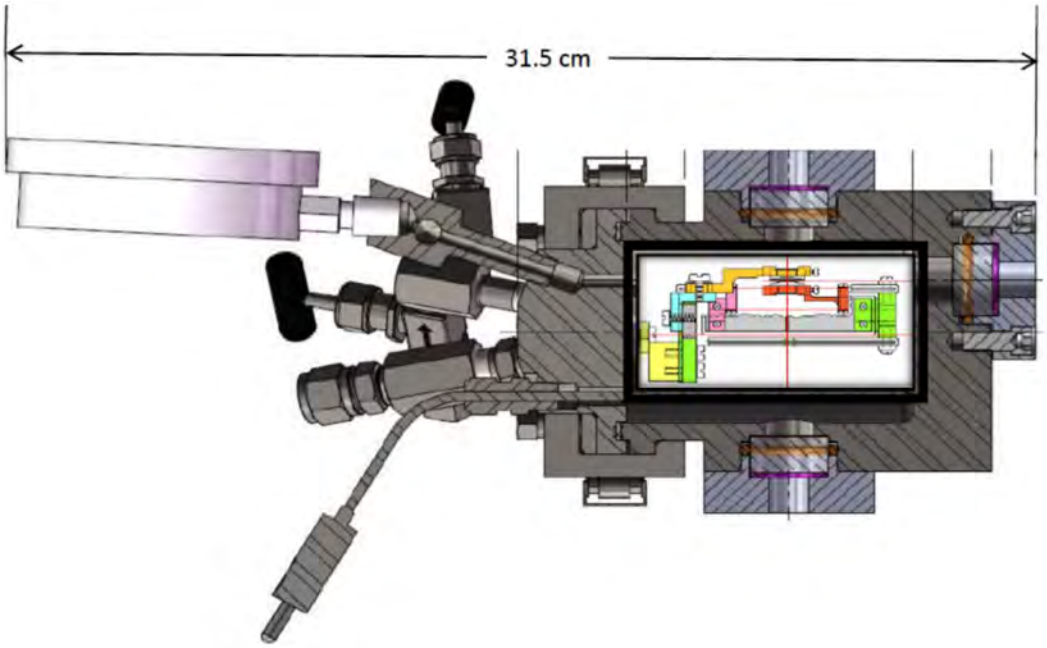

Figure 4—Schematic design of the HTHP-SFA with a custom designed SFA. The custom designed SFA, see details Figure 5, is placed inside a pressure vessel from Parr Instrument.

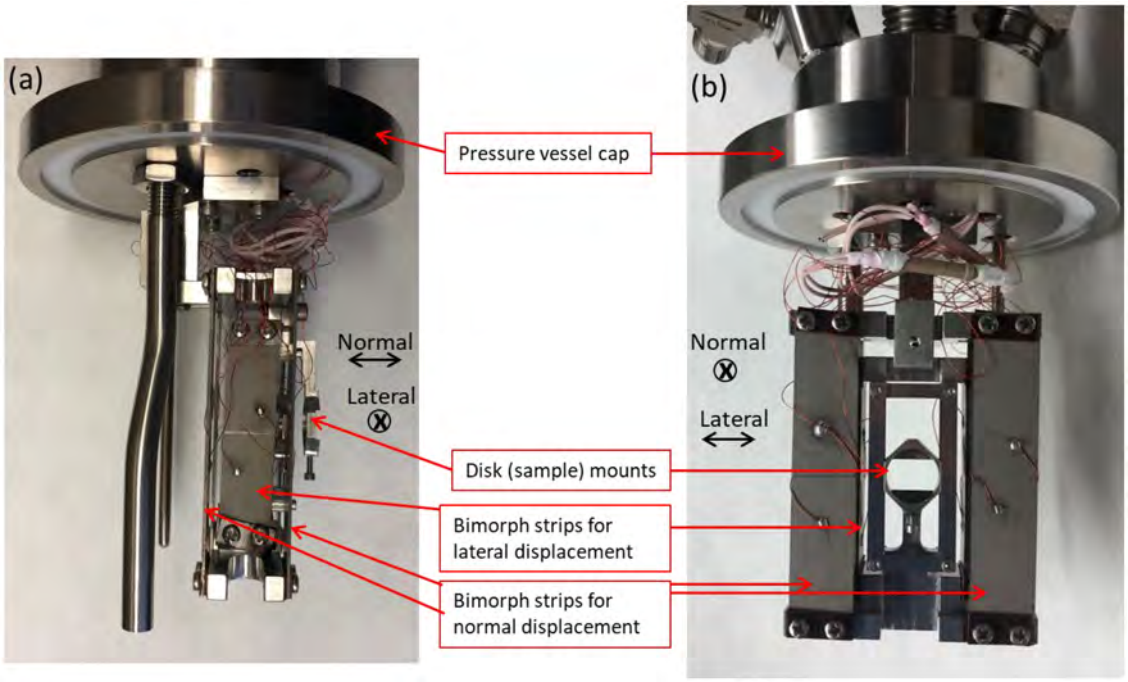

Figure 5—Details of the custom designed SFA in the HTHP-SFA. Photo of two views of the SFA insert of the HTHP-SFA. The SFA insert consists of piezoelectric (bimorph) strips for lateral and normal displacement of two apposing surface samples, and is attached to the pressure vessel cap. The electrical wires through the pressure vessel cap are connected to the bimorph strips that are used to control the displacement. The normal displacement is 1.4 μm/V and the lateral is 0.7 μm/V. The bimorph strips are electrically exposed and will need to be coated for electrical insulation before next phase of the project.

The SFA experiment were carried out with calcite surfaces in contact for the duration of the experiment. Ideally, the surfaces should be separated by a few micrometers between each data collection. Despite this limitation we nevertheless found interesting and unexpected results, see Results.

The next phase of the HTHP-SFA fabrication is to make the displacement mechanism of the SFA insert fully functional (see Figure 5). The displacement mechanism involves using piezoelectric (bimorph) strips for both the normal and lateral displacements. The bimorph strips are connected to the outside of the pressure vessel using electrical wires going through the pressure vessel cap. Since the experiments require electrolyte solutions, the bimorph strips and the connecting electrical wires need to be electrically insulated using an appropriate coating (i.e., a flexible polymer) that can withstand heat to 150°C.

A detailed summary of the experiments. The interferometric technique used in the SFA to measure calcite film thickness and roughness (i.e., minimum and maximum thicknesses) is thoroughly described in Chen *et al.*[25].

The preparation of aged calcite surfaces follows the procedure described in Chen *et al.*[23]. Here we provide the main steps. Calcite was deposited from solution onto mica substrates and fully-aged in CO-FW solution, as described in section 2.1.2. After aging, the calcite surfaces were transferred to the HTHP-SFA and kept in close contact at 2-3 atm lithostatic pressure for the duration of the experiment. We use calcite-calcite configuration (not mica-calcite) so as to avoid any possible pressure dissolution effects due to dissimiliar surfaces[27]. The surfaces will be in contact with solution even though the separation distance is only a few nanometers. During each measurement we first elevated temperature from room temperature to 50°C and then increased the hydrostatic pressure from 1 atm to 2000 PSI (using nitrogen gas) to mimic reservoir conditions. For the SmartWater experiment, the initial aged calcite thickness is 170 nm with 10 nm roughness. For the high salinity water (HSW) experiment, the initial aged calcite thickness is 120 nm with 20 nm roughness. The uncertainties in SFA data points is 5 nm.

Results and Discussion

Previous results on SmartWater effect[23-25] showed aged-calcite thinning due to (1) Flake removal and (2) Calcite roughening. We hypothesize that the same mechanism is valid for waterflooding under high pressure (2000 PSI) and elevated temperatures (50°C). To test this hypothesis, a new SFA that works at high hydrostatic pressures and elevated temperatures was designed. Using this new high temperature high pressure SFA (HTHP-SFA), waterflooding of high salinity water (HSW) and SmartWater were performed, see Figure 6 and 7. These experiments are compared to previous results on HSW and SmartWater performed at atmospheric pressures and similar temperatures.

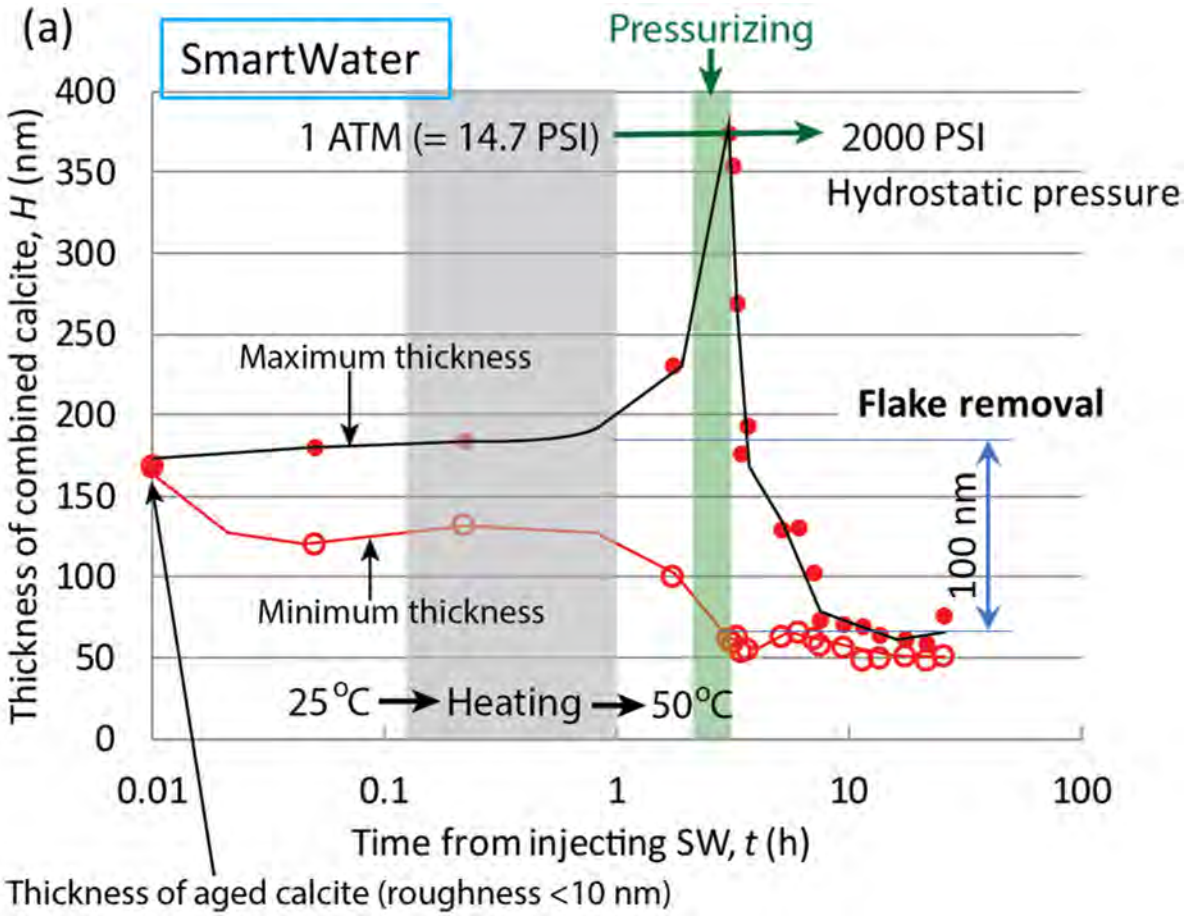

Figure 6—Changes in the maximum and minimum thickness of a pair of calcite surfaces as function of time in SmartWater. After the calcite surfaces were inserted, the SFA chamber was heated up to 50°C. After two hours, the SFA chamber was pressurized from atmospheric pressure to 2000 PSI. An unexpected increase of the maximum thickness during increase in hydrostatic pressure was observed. At high pressures the SmartWater effectively removes add-layers (flakes), resulting in a decrease in thickness leaving behind a smooth surface. The saturation index of calcite in SmartWater (1 atm, 100°C) is -2.1.

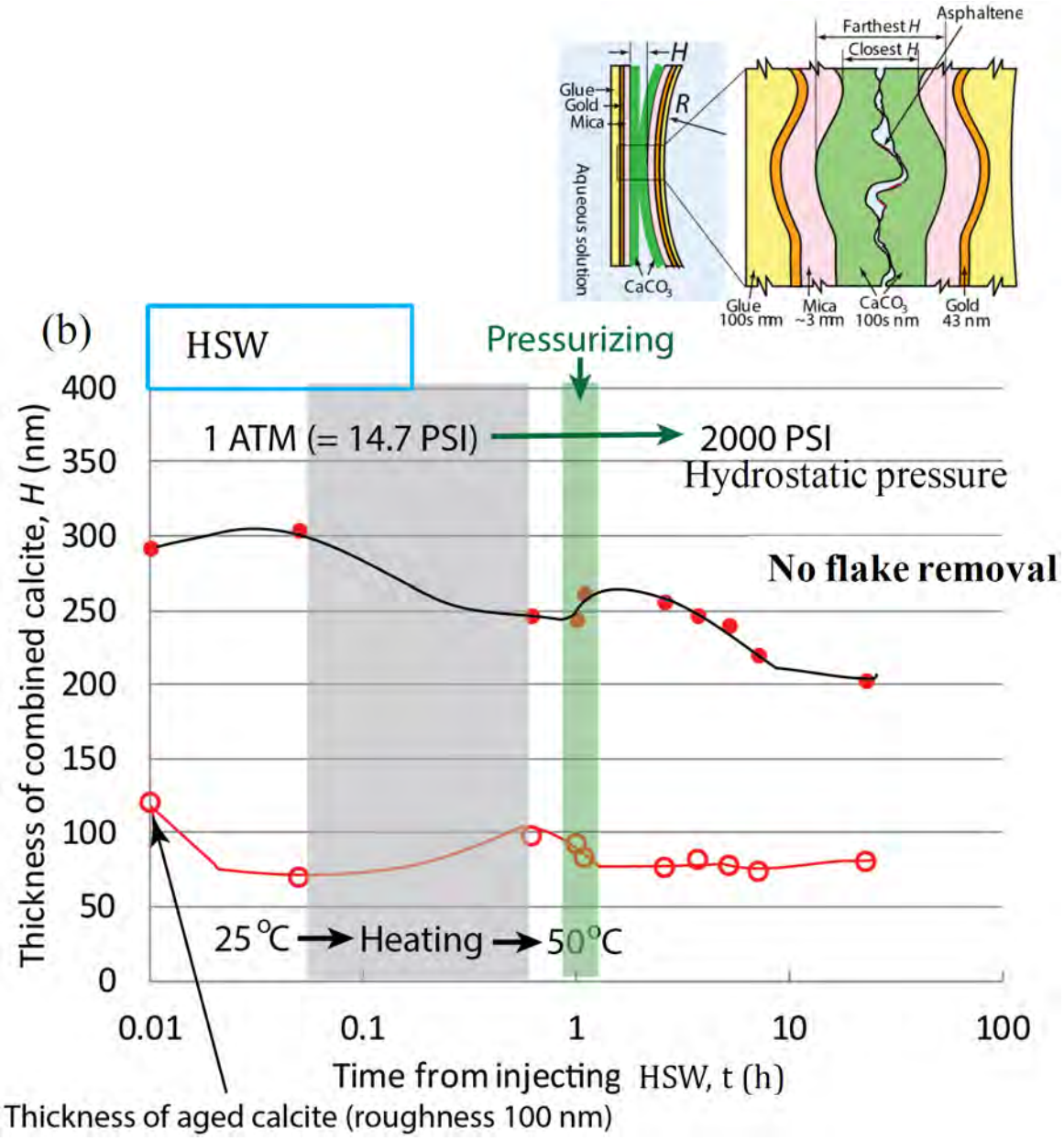

Figure 7—Changes in the maximum and minimum thickness of a pair of calcite surfaces (see inset) as function of time in HSW. After the calcite surfaces were inserted, the SFA chamber was heated up to 50°C. After one hour, the SFA chamber was pressurized from atmospheric pressure to 2000 PSI. HSW does not remove add-layers, resulting in no significant thickness change. The saturation index of calcite in HSW (1 atm, 100°C) is -0.5.

The new HTHP-SFA experiments monitoring changes in the calcite thickness and roughness under high pressure show a significant difference between SmartWater and HSW flooding. During SmartWater flooding, Figure 6, a high flake removal rate, manifested as a significant change in the layer maximum thickness. In addition, there is an unexpected degree of smoothening, that is, a small difference between the maximum and minimum thicknesses of calcite, as compared to experiments performed at atmosphereic pressure. The change in maximum thickness is 100 nm, which agrees well with our hypothesized flake removal process observed for SmartWater at 1 atm of 90 nm. Figure 7 shows that HSW flooding does not remove flakes from the aged calcite surface under high pressure.

We propose a possible explanation: (i) Dissolution is due to undersaturation of the aqueous solution, leading to precipitation outside contact region. The saturation indices of calcite (1 atm, 75°C) are -0.5 and -2.1 in HSW and SmartWater, respectively, which would predict greater dissolution in SmartWater.

Hydrostatic pressure has an unexpected effect. Note that these experiments are the first *in situ* quantitative measurement (first-of-its-kind). Further detailed measurements are needed to unravel this unexpected hydrostatic effect on aged calcite.

(ii) Another possible explanation includes flushing out of salt crystals from contact region (e.g., Na_2SO_4), which can be ruled out since we don't see any difference in HSW and SmartWater (i.e., 10-times reduced ions concentration HSW) flooding, and pressure dissolution effect can be ruled out since two similar surfaces do not show this effect.

To acquire a more detailed understanding of the mechanisms of calcite morphological changes and flake removal under reservoir conditions, more HTHP-SFA experiments are needed, which includes testing solutions with other salt concentrations. The above-mentioned experiments need to be accompanied by imaging and element analysis of single surface before and after exposure to high pressure. Contact angle measurements of a single aged calcite surfaces under high pressure and high temperature before and after flooding will quantify the wetting properties under reservoir conditions.

Conclusions

A new SFA that works under realistic reservoir conditions of high temperature and high-pressure conditions (up to 150°C and 2,200 psi) has been designed with the aim to study SmartWater effect – the increased oil recovery by waterflooding – at molecular and microscopic scale. First ever experiments on SmartWater flooding showed an unexpected effect of pressure on flake removal and calcite smoothening. In contrast, the results of high salinity water (HSW) flooding experiment indicated insignificant impact on removing flakes from the aged calcite surface under high pressure. These interesting results will require a new explanation for increased oil recovery in SmartWater flooding at high pressures.

Acknowledgements

This work was supported by ASC Contract No. Z-0038-2014 from Saudi Aramco. K.K. was partly supported by the Department of Energy, Office of Basic Energy Sciences, Division of Materials Sciences and Engineering, under Award DE-FG02-87ER-45331.

References

1. McGuire, P. L.; Chatham, J. R.; Paskvan, F. K.; Sommer, D. M.; Carini, F. H. Low Salinity Oil Recovery: An Exciting New EOR Opportunity for Alaska's North Slope, Paper SPE93903 presented at the 2005 SPE Western Regional Meeting held in Irvine, California, USA, 30 March - 1 April, 2005.
2. Seccombe, J.; Lager, A.; Jerauld, G.; Jhaveri, B.; Buikema, T.; Bassler, S.; Denis, J.; Webb, K.; Cockin, A.; Fueg, E. Demonstration of Low-Salinity EOR at Interwell Scale, Endicott Field, Alaska, Paper SPE 129692 presented at the 2010 SPE Improved Oil Recovery Symposium held in Tulsa, Oklahoma, USA, 24-28 April, 2010.
3. Webb, K. J.; Black, C. J. J.; Al-Ajeel, H. Low Salinity Oil Recovery - Log-Inject-Log, Paper 89379 presented at the SPE/DOE 14th Symposium on Improved Oil Recovery held in Tulsa, Oklahoma, USA, 17-21 April, 2004.
4. Webb, K. J.; Black, C. J. J.; Edmonds, L. J. Low Salinity Oil Recovery: The Role of Reservoir Condition Corefloods, Presented at the 13th European Symposium on Improved Oil Recovery held in Budapest, Hungary, 25-27 April, 2005.
5. Austad, T.; Strand, S.; Hognesen, E. J.; Zhang, P. Seawater as IOR Fluid in Fractured Chalk, Paper SPE 93900 presented at the SPE International Symposium on Oilfield Chemistry held in Houston, Texas, USA, 2-4 February, 2005.

6. Chandrasekhar, S.; Mohanty, K. K. Wettability Alteration with Brine Composition in High Temperature Carbonates Reservoirs, Paper SPE 166280 presented at the SPE Annual Technical Conference and Exhibition held in New Orleans, Louisiana, USA, 30 September - 2 October, 2013.
7. Gupta, R.; Mohanty, K. K., Wettability Alteration Mechanism for Oil Recovery from Fractured Carbonate Rocks. *Transport Porous Med* 2011, **87** (2), 635–652.
8. Gupta, R.; Smith, P. G., Jr.; Hu, L.; Willingham, T. W.; Cascio, L. M.; Shyeh, J. J.; Harris, C. R. Enhanced Waterflood for Middle East Carbonate Cores - Impact of Injection Water Composition, Paper SPE 142668 presented at the SPE Middle East Oil and Gas Show and Conference held in Manama, Bahrain, 25-28 September, 2011.
9. Webb, K. J.; Black, C. J. J.; Tjetland, G. A. A Laboratory Study Investigating Methods for Improved Oil Recovery in Carbonates, Paper IPTC 10506 presented at the International Petroleum Technology Conference held in Doha, Qatar, 21-23 November, 2005.
10. Yousef, A. A.; Al-Saleh, S. H.; Al-Kaabi, A.; Al-Jawfi, S. M., Laboratory investigation of the impact of injection-water salinity and ionic content on oil revocery from carbonate reservoirs. *SPE Reservoir Evaluation & Engineering* 2011, **14** (05), 578–593.
11. Yousef, A. A.; Liu, J. S.; Blanchard, G. W. Smart Waterflooding: Industry's First Field Test in Carbonate Reservoirs, Paper SPE 159526 presented at the SPE Annual Technical Conference and Exhibition held in San Antonio, Texas, USA, 8-10 October, 2012.
12. Ayirala, S. C.; Boqmi, A.; Alghamdi, A.; Al-Sofi, A., Dilute surfactants for wettability alteration and enhanced oil recovery in carbonates. *Journal of Molecular Liquids* 2019, **285**, 707–715.
13. Han, M.; AlSofi, A.; Fuseni, A.; Zhou, X.; Hassan, S. Development of Chemical EOR Formulations for a High Temperature and High Salinity Carbonate Reservoir, Paper IPTC 17084 presented at the International Petroleum Technology Conference, Beijing, China, 26-28 March, 2013.
14. Iglauer, S.; Wu, Y. F.; Shuler, P.; Tang, Y. C.; Goddard, W. A., New surfactant classes for enhanced oil recovery and their tertiary oil recovery potential. *J Petrol Sci Eng* 2010, **71** (1-2), 23–29.
15. Lu, J.; Goudarzi, A.; Chen, P. L.; Kim, D. M.; Delshad, M.; Mohanty, K. K.; Sepehrnoori, K.; Weerasooriya, U. P.; Pope, G. A., Enhanced oil recovery from high-temperature, high-salinity naturally fractured carbonate reservoirs by surfactant flood. *J Petrol Sci Eng* 2014, **124**, 122–131.
16. Nwidee, L. N.; Theophilus, S.; Barifcani, A.; Sarmadivaleh, M.; Iglauer, S., EOR Processes, Opportunities and Technological Advancements. *Chemical Enhanced Oil Recovery (cEOR) - A Practical Overview*, Romero-Zeron, L., Ed. InTech: 2016; pp 2–52.
17. Seethepalli, A.; Adibhatla, B.; Mohanty, K. K., Physicochemical interactions during surfactant flooding of fractured carbonate reservoirs. *Spe J* 2004, **9** (4), 411–418.
18. Lager, A.; Webb, K. J.; Black, C. J. J.; Singleton, M.; Sorbie, K. S., Low salinity oil recovery - An experimental investigation. *Petrophysics* 2008, **49** (1), 28–35.
19. Morrow, N. R.; Tang, G. Q.; Valat, M.; Xie, X., Prospects of improved oil recovery related to wettability and brine composition. *J Petrol Sci Eng* 1998, **20** (3-4), 267–276.
20. Mugele, F.; Siretanu, I.; Kumar, N.; Bera, B.; Wang, L.; de Ruiter, R.; Maestro, A.; Duits, M.; van den Ende, D.; Collins, I., Insights From Ion Adsorption and Contact-Angle Alteration at Mineral Surfaces for Low-Salinity Waterflooding. *SPE J* 2016, **21** (4), 1204–1213.
21. Yildiz, H. O.; Morrow, N. R., Effect of brine composition on recovery of Moutray crude oil by waterflooding. *J Petrol Sci Eng* 1996, **14** (3-4), 159–168.
22. Myint, P. C.; Firoozabadi, A., Thin liquid films in improved oil recovery from low-salinity brine. *Curr Opin Colloid* In 2015, **20** (2), 105–114.

23. Chen, S. Y.; Kaufman, Y.; Kristiansen, K.; Seo, D. J.; Schrader, A. M.; Alotaibi, M. B.; Dobbs, H. A.; Cadirov, N. A.; Boles, J. R.; Ayirala, S. C.; Israelachvili, J. N.; Yousef, A. A., Effects of Salinity on Oil Recovery (the "Dilution Effect"): Experimental and Theoretical Studies of Crude Oil/Brine/Carbonate Surface Restructuring and Associated Physicochemical Interactions. *Energ Fuel* 2017, **31** (9), 8925–8941.
24. Chen, S.-Y.; Kaufman, Y.; Kristiansen, K.; Dobbs, H. A.; Cadirov, N. A.; Seo, D.; Schrader, A. M.; Andresen Eguiluz, R. C.; Alotaibi, M. B.; Ayirala, S. C.; Boles, J. R.; Yousef, A. A.; Israelachvili, J. N. New Atomic to Molecular Scale Insights Into SmartWater Flooding Mechanisms in Carbonates, Paper SPE 190281 presented at the SPE Improved Oil Recovery Conference held in, Tulsa, Oklahoma, USA, 14 - 18 April; Tulsa, Oklahoma, USA, 2018.
25. Chen, S. Y.; Kristiansen, K.; Seo, D.; Cadirov, N. A.; Dobbs, H. A.; Kaufman, Y.; Schrader, A. M.; Eguiluz, R. C. A.; Alotaibi, M. B.; Ayirala, S. C.; Boles, J. R.; Yousef, A. A.; Israelachvili, J. N., Time-Dependent Physicochemical Changes of Carbonate Surfaces from SmartWater (Diluted Seawater) Flooding Processes for Improved Oil Recovery. *Langmuir* 2019, **35** (1), 41–50.
26. Israelachvili, J.; Min, Y.; Akbulut, M.; Alig, A.; Carver, G.; Greene, W.; Kristiansen, K.; Meyer, E.; Pesika, N.; Rosenberg, K.; Zeng, H., Recent advances in the surface forces apparatus (SFA) technique. *Rep Prog Phys* 2010, **73** (3), 036601.
27. Kristiansen, K.; Valtiner, M.; Greene, G. W.; Boles, J. R.; Israelachvili, J. N., Pressure solution - The importance of the electrochemical surface potentials. *Geochim Cosmochim Acta* 2011, **75** (22), 6882–6892.